The Gd^{3+} Complex of a Fatty Acid Analogue of DOTP Binds to Multiple Albumin Sites with Variable Water Relaxivities

Peter Caravan,[†] Matthew T. Greenfield,[†] Xiaodong Li,[‡] and A. Dean Sherry*[,‡,§]

EPIX Medical, 71 Rogers Street, Cambridge, Massachusetts 02142, Department of Chemistry, University of Texas at Dallas, Richardson, Texas 75083, and Department of Radiology, Rogers Magnetic Resonance Center, University of Texas Southwestern Medical Center, 5801 Forest Park Road, Dallas, Texas 75290

Received March 16, 2001

The 20 MHz water relaxivity (r_1) of gadolinium(III) complexes formed with two fatty acid analogues of 1,4,7,-10-tetraazacyclododecane-1,4,7,10-tetrakis(methylene phosphonate) were shown to increase substantially in the presence of albumin. The r_1 values of Gd(C_8-DOTP)$^{5-}$ and Gd(C_{11}-DOTP)$^{5-}$ in water were similar to that of the parent GdDOTP^{5-}, a $q = 0$ complex known to relax water very efficiently via an outer-sphere mechanism. Neither fatty acid analogue formed apparent aggregates or micelles in water up to 20 mM, but both showed dramatic increases in r_1 upon addition of albumin. Further ultrafiltration studies of Gd(C_{11}-DOTP)$^{5-}$ in the presence of non-defatted HSA showed that the complex binds at a minimum of five high-affinity fatty acid sites with stepwise binding constants ranging from 1.27×10^5 to 2.7×10^3 M^{-1}. The 20 MHz relaxivity of Gd(C_{11}-DOTP)$^{5-}$ in the presence of excess HSA was 23 mM^{-1} s^{-1} at 25 °C. The NMRD curve showed a broad maximum 20−30 MHz which fitted well to standard theory for a $q = 0$ complex with rapid outer-sphere water exchange. The r_{1b} of Gd(C_{11}-DOTP)$^{5-}$ bound at the tightest site on HSA was ∼40 mM^{-1} s^{-1} at 5 °C, an extraordinarily high value for an outer-sphere complex. However, the r_{1b} of Gd(C_{11}-DOTP)$^{5-}$ bound at the weaker sites on HSA was considerably lower, approaching the relaxivity of the free complex in water. This suggests that the complex bound in the highest affinity fatty acid site is less mobile than the same complex bound at the weaker affinity fatty acid sites. This combined ultrafiltration and relaxivity study demonstrates that the common assumption of a single r_{1b} value for a Gd^{3+} complex bound at several protein sites is not a valid approximation.

Introduction

Efforts to substantially increase the water relaxivity (r_1) of low molecular weight Gd^{3+} complexes by attaching them to larger structures that undergo slow rotation has so far been limited either by water exchange or chelate flexibility.[1,2] Water exchange in the uncomplexed Ln^{3+} aquo ions is known to be fast (the water lifetime, τ_M, is ∼1−10 ns[3,4]) so fast water exchange was assumed in the first generation MRI contrast agents, GdDTPA^{2-} and GdDOTA$^-$, as well. Later, however, Micskei et al.[5] found that τ_M is much longer in $q = 1$ complexes than anticipated (about 200 ns for GdDOTA$^-$ and GdDTPA^{2-}) and that exchange occurs via a dissociative mechanism.[6] Upon attachment of these complexes to a macromolecule, rotation does slow as anticipated but r_1 does not reach the theoretical maximum (greater than 100 mM^{-1} s^{-1} for a $q = 1$ complex)[2] either because the attached chelate is too flexible (internal motions dominate τ_R) or water exchange becomes limiting ($\tau_M > T_{1M}$). For example, a GdDTPA^{2-} derivative having a hydrophobic side chain that binds moderately to human serum albumin (MS-325) shows a 9-fold increase in r_1 (to ∼51 mM^{-1} s^{-1} at 20 MHz, 37 °C) upon binding to the protein[7−9] while the maximum r_1 reached by GdDOTA$^-$ derivatives bound to dendimers[10] of increasing size is ∼45 mM^{-1} s^{-1}. Furthermore, GdDTPA^{2-} or GdDOTA$^-$ conjugated to polylysine of various molecular weights results in conjugates having even lower r_1 values (∼13 mM^{-1} s^{-1}),[11,12] likely reflecting the greater mobility of polylysine side chains rather than limits imposed by water exchange. Aime et al.[13] recently reported that GdDO3A(BOM)$_3$, a $q = 2$ complex with more favorable but still not optimal water exchange, has a r_{1b} of 80 mM^{-1} s^{-1} (20 MHz, 25 °C) when

* Author to whom correspondence should be sent to either address. Telephone: 972-883-2907 or 214-648-5877. Fax: 972-883-2925 or 214-648-5881. E-mail: sherry@utdallas.edu or dean.sherry@utsouthwestern.edu.
[†] EPIX Medical.
[‡] University of Texas at Dallas.
[§] University of Texas Southwestern Medical Center.

(1) Caravan, P.; Ellison, J. J.; McMurry, T. J.; Lauffer, R. B. *Chem. Rev.* **1999**, *99*, 2293−2352.
(2) Aime, S.; Botta, M.; Fasano, M.; Terreno, E. *Chem. Soc. Rev.* **1998**, *27*, 19−29.
(3) Southwood-Jones, R. V.; Earl, W. L.; Newman, K. E.; Merbach, A. E. *J. Chem. Phys.* **1980**, *73*, 5909−5918.
(4) Cossy, C.; Helm, L.; Merbach, A. E. *Inorg. Chem.* **1988**, *27*, 1973−1979.
(5) Micskei, K.; Helm, L.; Brucher, E.; Merbach, A. E. *Inorg. Chem.* **1993**, *32*, 3844−3850.
(6) Powell, D. H.; Ni Dhubhghaill, O. M.; Pubanz, D.; Lebedev, Y.; Schlaepter, W.; Merbach, A. E. *J. Am. Chem. Soc.* **1996**, *118*, 9333−9346.
(7) Muller, R. N.; Radüchel, B.; Laurent, S.; Platzek, J.; Piérart, C.; Mareski, P.; Vander Elst, L. *Eur. J. Inorg. Chem.* **1999**, 1949−1955.
(8) Lauffer, R. B.; Parmelee, D. J.; Dunham, S. U.; Ouellet, H. S.; Dolan, R. P.; Witte, S.; McMurry, T. J.; Walovitch, R. C. *Radiology* **1998**, *207*, 529−538.
(9) Aime, S.; Botta, M.; Frullano, L.; Crich, S. G.; Giovenzana, G. B.; Pagliarin, R.; Palmisano, G.; Sisti, M. *Chem. Eur. J.* **1999**, *5*, 1253−1260.
(10) Bryant, L. H., Jr.; Brechbiel, M. W.; Wu, C.; Bulte, J. W. M.; Herynek, V.; Frank, J. A. *J. Magn. Reson. Imaging* **1999**, *9*, 348−352.
(11) Schuhmann-Giampiere, G.; Schmitt-Willich, H.; Frenzel, T.; Press, W. R.; Weinmann, H. J. *Invest. Radiol.* **1991**, *26*, 969−974.
(12) Sieving, P. F.; Watson, A. D.; Rocklage, S. M. *Bioconjugate Chem.* **1990**, *1*, 65−71.
(13) Aime, S.; et al. Presented at the XIX International Conference on Magnetic Resonance in Biological Systems; Florence, Italy, August 2000.

10.1021/ic0102900 CCC: $20.00
Published on Web 12/10/2001

Chart 1

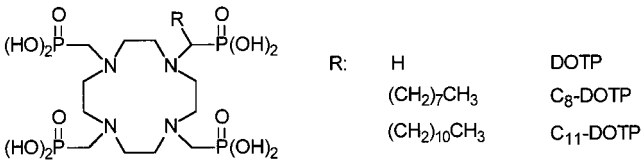

bound to a cross-linked β-cyclodextrin. This demonstrates that a Gd^{3+} complex having an optimal water exchange rate ($\sim$30 ns) might indeed display a r_{1b} that approaches the theoretical maximum upon binding to a macromolecule.

One way to avoid the limitations imposed by inner-sphere water exchange is to use a Gd complex that binds efficiently to a larger number of outer-sphere (i.e., second coordination sphere) water molecules. One suitable candidate complex is $GdDOTP^{5-}$. This low molecular weight complex does not have an available inner-sphere coordination site for water yet displays a 20 MHz r_1 relaxivity higher than that of $GdDOTA^-$ ($q = 1$).[14,16] In an effort to design a sodium shift reagent (SR) with improved hyperfine shift features and reduced in vivo clearance rate, we recently set out to add hydrophobic substituents to DOTP, a ligand widely used as a SR for ^{23}Na MR (magnetic resonance).[18−22] In a companion paper,[23] we characterized lanthanide complexes of 1-(1-octyl-methyl-phosphonic acid)-4,7,10-tris(methylene phosphonic acid)-1,4,7,10-tetraazacyclododecane (C_8-DOTP, Chart 1) and 1-(1-undecyl-methyl-phosphonic acid)-4,7,10-tris(methylene phosphonic acid)-1,4,7,-10-tetraazacyclododecane (C_{11}-DOTP, Chart 1) and found that the complexes were more rigid in solution than the parent DOTP complexes and consequently induce larger hyperfine shifts in ^1H NMR spectra of their Ln^{3+} complexes and in the ^{23}Na spectrum of ion-paired Na^+ ions. Preliminary experiments showed that lanthanide complexes of both ligands interact strongly with albumin. Here, we report a detailed investigation of the binding of the most hydrophobic complex, $Gd(C_{11}\text{-DOTP})^{5-}$, with albumin and examine the consequences of binding on the r_1 of the complex.

Experimental Section

Preparation of Ligands. The synthetic route to C_{11}-DOTP and C_8-DOTP is described in a companion paper.[23] The Gd^{3+} complexes were prepared by mixing a stock solution of $GdCl_3$ with a solution of ligand (5−10% molar excess) at pH 8−9 and $\sim$65 °C. The pH was adjusted as necessary with NaOH for a period of $\sim$1 h. The solution was then freeze-dried to a white powder and the complex redissolved into water or buffer at the appropriate concentration for further studies. Gadolinium concentrations were determined by ICP-MS with a PE-SCIEX ELAN 5000.

Water Relaxation Rates. The relaxivity of $Gd(C_{11}\text{-DOTP})^{5-}$ was determined in water and in 4.5% (w/v) bovine serum albumin at 20 MHz using a MRS-6 NMR analyzer (Institut Jozef Stefan, Ljuljana, Slovenija) with the temperature controlled at 25 °C using a stream of dry air. Relaxivity values measured on samples after ultrafiltration were collected using a Bruker NMS 120 minispec at 37 °C. T_1 was measured with an inversion recovery pulse sequence on both instruments. The T_1 NMRD profiles were recorded on a Koenig-Brown relaxometer from 0.01 to 50 MHz.

Preparation of Human Serum Albumin (HSA). Fraction V HSA (Sigma, not defatted) was dissolved in PBS buffer containing 10 mM sodium phosphate and 150 mM sodium chloride (pH 7.4). The protein concentration was determined by measuring its absorbance at 280 nm and comparing the readings to a standard curve constructed from the absorbance of HSA standards (Sigma) in PBS buffer. An HSA molecular weight of 66435 Da was used to convert % (w/v) to a molar concentration.

Binding of $Gd(C_{11}\text{-DOTP})^{5-}$ to HSA. Gd complex/protein samples ranging from 0.023 mM to 1.32 mM GdL and 0.023 mM (0.16%) to 0.667 mM (4.5%) HSA were prepared. Aliquots (400 μL) of these samples were placed in ultrafiltration units (Millipore Corporation, 30000 MW cutoff), incubated at 37 °C for 20 min, and then centrifuged at 3500 g for 7 min. Control experiments established that GdL did not bind to the membrane. It was assumed that GdL bound to HSA would not pass through the MW cutoff filter and that the filtrate that passed through the filter accurately represented the free concentration of GdL in each sample. Duplicate aliquots were processed for each concentration. Concentrations of total GdL in the initial solutions containing protein and in the filtrates were determined by measuring Gd^{3+} using ICP-MS.

Displacement of Dansylsarcosine (DS) by $Gd(C_{11}\text{-DOTP})^{5-}$. A solution containing [DS] $\sim$ [HSA] $\sim$ 5 μM plus 100 μM GdL was prepared. Aliquots of this solution were 2-fold diluted serially by addition of a second solution containing the same concentrations of DS and HSA but no GdL, to produce eight samples of differing [GdL]. The fluorescence of 100 μL aliquots of each of these samples was measured in quadruplicate in 96 well plates. Sixteen 100 μL aliquots of the solution containing no GdL (maximum fluorescent intensity) were also measured in the same 96-well plate, along with 16 100 μL aliquots of HSA in PBS (minimum fluorescent intensity). These two controls set the dynamic range for the observed fluorescence. The inhibition constant, K_i, of GdL was determined using eqs 1 and 2. Given the known binding constant of DS with HSA ($K_d = 5$ μM), $[DS]_{bound}$ was determined from the fluorescence data and an apparent (in the presence of GdL) K_d^{app} for DS was determined. The inhibition constant for GdL was determined from eq 2.

$$[DS]_{bound} = \frac{([HSA]_t + [DS]_t + K_d^{app}) - \sqrt{([HSA]_t + [DS]_t + K_d^{app})^2 - 4[HSA]_t[DS]_t}}{2} \quad (1)$$

$$K_d^{app} = K_d(1 + [GdL]_{free}/K_i) \quad (2)$$

Results

The paramagnetic contribution to the water relaxation rate ($1/T_{1p} = R_{1p}$) increases linearly with concentration up to 20 mM for $Gd(C_8\text{-DOTP})^{5-}$ and $Gd(C_{11}\text{-DOTP})^{5-}$ (Figure 1). The linearity of these plots is consistent with complexes that do not aggregate in water below 20 mM. The 20 MHz relaxivity values determined from the slopes of these lines were 5.12 and 4.60 $mM^{-1}\ s^{-1}$ for the octyl- and undecyl derivatives, respectively. These values are similar to the 20 MHz, 25 °C value reported for $GdDOTP^{5-}$, a complex known to lack an inner-sphere water coordination site.[15] The unusually high relaxivity of the latter

(14) Aime, S.; Botta, M.; Terreno, E.; Anelli, P. L.; Uggeri, F. *Magn. Res. Med.* **1993**, *30*, 583−591.
(15) Sherry, A. D.; Ren, J.; Huskens, J.; Brucher, E.; Toth, E.; Geraldes, C. F. G. C.; Castro, M. M. C. A.; Cacheris, W. P. *Inorg. Chem.* **1996**, *35*, 4604−4612.
(16) Botta, M. *Eur. J. Inorg. Chem.* **2000**, 399−407.
(17) Alpoim, M. C., Urbano, A. M., Geraldes, C. F. G. C. , Peters, J. A. *J. Chem. Soc., Dalton Trans.* **1992**, 463−467.
(18) Bansal, N.; Germann, M. J.; Seshan, V.; Shires, G. T., III; Malloy, C. R.; Sherry, A. D. *Biochemistry* **1993**, *32*, 5638−5643.
(19) Pike, M. M.; Luo, C. S.; Clark, M. D.; Kirk, K.; Kitakaze, M.; Madden, M. C.; Gragoe, E. J., Jr.; Pohost, G. M. *Am. J. Physiol.* **1993**, *265*, H2017−H2026.
(20) Seshan, V.; Germann, M. J.; Preisig, P.; Malloy, C. R.; Sherry, A. D.; Bansal, N. *Magn. Reson. Med.* **1995**, *34*, 25−31.
(21) Van Emous, J. G.; Schreur, J. H. M.; Ruigrok, T. J. C.; Van Echteld, C. J. A. *J. Mol. Cell. Cardiol.* **1998**, *30*, 337−348.
(22) Colet, J.-M.; Makos, J. D.; Malloy, C. R.; Sherry, A. D. *Magn. Reson. Med.* **1998**, *39*, 155−159.
(23) Li, X.; Zhang, S.; Zhao, P.; Kovacs, Z.; Sherry, A. D. *Inorg. Chem.* **2001**, *40*, 6572−6579.

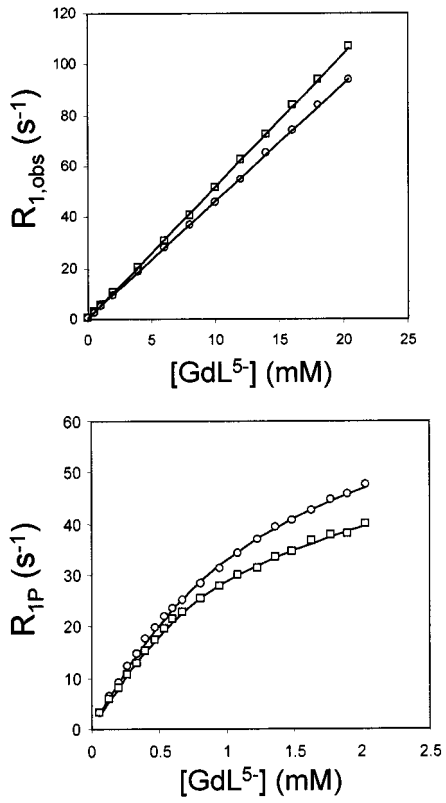

Figure 1. Paramagnetic relaxation rate of as a function of $Gd(C_8\text{-}DOTP)^{5-}$ (□) or $Gd(C_{11}\text{-}DOTP)^{5-}$ (○) concentration in water (left) and in a 4.5% BSA (right), 25 °C, 20 MHz. The solid lines represent a linear fit of the data (left) or a fit of the data to eq 4 (right).

complex has been ascribed to an association of an unknown number of second coordination sphere water molecules with the highly charged tetraphosphonate surface of this complex.[14,16] The ^{17}O NMR method[17] was used to verify that $Dy(C_8\text{-}DOTP)^{5-}$ does not have an inner-sphere water coordination site. This formed the basis of the assumption that, like $GdDOTP^{5-}$, neither $Gd(C_8\text{-}DOTP)^{5-}$ nor $Gd(C_{11}\text{-}DOTP)^{5-}$ has an inner-sphere exchanging water molecule.

Figure 1 also shows relaxation curves for $Gd(C_8\text{-}DOTP)^{5-}$ and $Gd(C_{11}\text{-}DOTP)^{5-}$ when added to an aqueous solution containing 4.5% (w/v) fatty acid free BSA. The dramatic increase in R_{1p} over that seen in water likely reflects binding of these fatty acid analogues to sites on the protein, thereby slowing rotation of the complex. In the presence of albumin, R_{1p} has contributions from both the free, unbound chelate (r_{1f}) and the albumin-bound adduct (r_{1b}).

$$R_{1p} = r_{1f}[\text{GdL}]_f + r_{1b}[\text{GdL-BSA}] \quad (3)$$

If one assumes N independent and equivalent binding sites for $Gd(C_8\text{-}DOTP)^{5-}$ or $Gd(C_{11}\text{-}DOTP)^{5-}$ (abbreviated as GdL) on BSA, data such as this can be fitted using standard proton relaxation enhancement (PRE) assumptions:[24]

$$R_{1p} = 1000\{(r_{1f}S^0) + {}^1/_2(r_{1b} - r_{1f})((NP^0) + S^0 + K_a^{-1} - \sqrt{((NP^0) + S^0 + K_a^{-1})^2 - 4NS^0P^0})\} \quad (4)$$

Here, K_a is the association constant; S^0 and P^0 are the total molar concentrations of GdL and BSA, respectively. If one makes the oversimplifying assumption of a single binding site and fits the curves of Figure 1 to eq 4, one gets a $K_a = 4768 \pm 268$ and $r_{1b} = 54 \pm 1$ mM^{-1} s^{-1} for the $Gd(C_8\text{-}DOTP)^{5-}$ data and a $K_a = 2300 \pm 127$ and $r_{1b} = 77 \pm 1$ $mM^{-1}s^{-1}$ for the $Gd(C_{11}\text{-}DOTP)^{5-}$ data. In both cases, r_{1f} was assumed equal to the respective values measured in pure water. This approximation is valid since the BSA concentration used in this study (0.68 mM) is well below the 3.5 mM limit above which the effect of local microviscosity on water relaxation is no longer negligible for a globular protein.[25] Although these association constants are in the same range[26] as for other small Gd^{3+} complexes that bind to albumin, i.e., 10^2-10^5 M^{-1}, the r_{1b} values determined in this calculation are much higher than those anticipated for an outer-sphere complex bound to a protein. This suggested to us that the assumptions involved in this calculation are not correct and that more detailed binding studies were warranted.

Table 1. Binding of $Gd(C_8\text{-}DOTP)^{5-}$ and $Gd(C_{11}\text{-}DOTP)^{5-}$ (0.1 mM) to Defatted BSA (4.5%) and to Non-Defatted HSA (4.5%) at 37 °C, Single Point Affinity Estimates at 37 °C, and Apparent Relaxivities at 20 and 37 °C (20 MHz)

	% bound	K_a ($\times 10^{-3}$ M^{-1})[a]	r_1^{obs} (mM^{-1} s^{-1})	
			20 °C	37 °C
$Gd(C_8\text{-}DOTP)^{5-}$/HSA	89.3	14.4	20.38	15.82
$Gd(C_8\text{-}DOTP)^{5-}$/BSA	74.5	4.9	20.50	15.80
$Gd(C_{11}\text{-}DOTP)^{5-}$/HSA	99.3	249	28.67	19.86
$Gd(C_{11}\text{-}DOTP)^{5-}$/BSA	97.5	68.1	33.96	26.55

[a] Calculated assuming a single binding site and [protein] = 0.67 mM.

Ultrafiltration Experiments. Further albumin binding studies were performed with defatted bovine serum albumin (BSA) and non-defatted human serum albumin (HSA, fraction V). Protein−complex binding was determined by ultrafiltration through a membrane with a 30000 MW cutoff.[8] Total gadolinium in the GdL−protein mixture (representing total GdL) and in the filtrate (representing unbound GdL) were measured by ICP-MS. Initial studies were carried out on 0.1 mM $Gd(C_{11}\text{-}DOTP)^{5-}$ or $Gd(C_8\text{-}DOTP)^{5-}$ in the presence of 4.5% defatted BSA or non-defatted HSA (~0.67 mM protein) at 37 °C, and the observed relaxivities (a combination of free and bound) were measured at 20 MHz, 37 °C (Table 1). Table 1 shows that the affinity of the undecyl derivative is significantly higher than that of the octyl derivative and that binding to non-defatted HSA is more favorable than binding to defatted BSA for both complexes. The relaxivity determinations showed that $Gd(C_{11}\text{-}DOTP)^{5-}$ is a better protein-bound relaxation agent than $Gd(C_8\text{-}DOTP)^{5-}$ (also evident in the data of Figure 1) and that the relaxation enhancement increases with decreasing temperature. It is clear from Table 1 that the affinity of $Gd(C_{11}\text{-}DOTP)^{5-}$ for BSA estimated from the ultrafiltration experiment is much higher than the affinity estimated from the PRE study. Since the affinity and relaxivity determined from the PRE study are both model dependent, it was decided to study the binding and relaxation enhancement of $Gd(C_{11}\text{-}DOTP)^{5-}$ in more detail by both ultrafiltration and relaxation measurements.

Although the highest relaxivity was observed with defatted BSA, further studies were undertaken with non-defatted HSA since this was judged the most representative of plasma albumin. The extent of binding of $Gd(C_{11}\text{-}DOTP)^{5-}$ to HSA is shown in Figure 2. The total concentration of $Gd(C_{11}\text{-}DOTP)^{5-}$ ranged

(24) Vander Elst, L.; Laurent, S.; Botteman, F.; Muller, R. N. *Magn. Reson. Mater. Phys., Biol. Med.* **1998**, *6* (suppl.), 84.
(25) Koenig, S. H.; Brown, R. D., III. *Prog. Nucl. Magn. Reson. Spectrosc.* **1990**, *22*, 487−567.
(26) Aime, S.; Botta, M.; Fasano, M.; Crich, S. G.; Terreno, E. *Coord. Chem. Rev.* **1999**, *185−186*, 321−333.

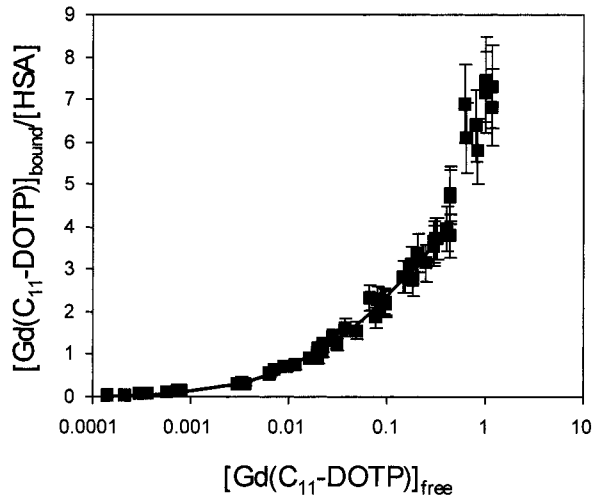

Figure 2. Plot demonstrating the binding capacity of non-defatted HSA (4.5%) for $Gd(C_{11}\text{-DOTP})^{5-}$ as determined by ultrafiltration studies at 37 °C. The plot shows no saturation out to 8 equiv of $Gd(C_{11}\text{-DOTP})^{5-}$ bound per HSA.

from 0.023 mM to 1.32 mM while the protein concentration varied from 0.023 mM (0.16%) to 0.667 mM (4.5%). Under these conditions the percent bound to HSA ranged from 99.3 (0.02 mM $Gd(C_{11}\text{-DOTP})^{5-}$, 0.667 mM HSA) to 11.9% (1.32 mM $Gd(C_{11}\text{-DOTP})^{5-}$, 0.023 mM HSA). The data are presented in Figure 2 as a plot of the ratio of bound $Gd(C_{11}\text{-DOTP})^{5-}$ per HSA molecule ($\bar{n}$) versus the concentration of unbound $Gd(C_{11}\text{-DOTP})^{5-}$. It is clear from Figure 2 that $\bar{n}$ increases steeply as the molar concentration (on a logarithmic scale) increases. It is apparent that saturation does not occur even at 8 mol of bound $Gd(C_{11}\text{-DOTP})^{5-}$ per HSA. It was possible to fit the data to a stoichiometric model[27] to estimate the first five stepwise binding constants.

$$\text{GdL} + \text{HSA} \rightarrow (\text{GdL})\text{HSA} \qquad K_{a1} = \frac{[(\text{GdL})\text{HSA}]}{[\text{GdL}][\text{HSA}]} \quad (5)$$

$$\text{GdL} + (\text{GdL})\text{HSA} \rightarrow (\text{GdL})_2\text{HSA} \qquad K_{a2} = \frac{[(\text{GdL})_2\text{HSA}]}{[\text{GdL}][(\text{GdL})\text{HSA}]} \quad (6)$$

$$\text{GdL} + (\text{GdL})_2\text{HSA} \rightarrow (\text{GdL})_3\text{HSA} \qquad K_{a3} = \frac{[(\text{GdL})_3\text{HSA}]}{[\text{GdL}][(\text{GdL})_2\text{HSA}]} \quad (7)$$

$$\text{GdL} + (\text{GdL})_3\text{HSA} \rightarrow (\text{GdL})_4\text{HSA} \qquad K_{a4} = \frac{[(\text{GdL})_4\text{HSA}]}{[\text{GdL}][(\text{GdL})_3\text{HSA}]} \quad (8)$$

$$\text{GdL} + (\text{GdL})_4\text{HSA} \rightarrow (\text{GdL})_5\text{HSA} \qquad K_{a5} = \frac{[(\text{GdL})_5\text{HSA}]}{[\text{GdL}][(\text{GdL})_4\text{HSA}]} \quad (9)$$

The function $\bar{n}$ can be expressed in terms of these five association constants by eq 10,

$$\bar{n} = \frac{\beta_1 F + 2\beta_2 F^2 + 3\beta_3 F^3 + 4\beta_4 F^4 + 5\beta_5 F^5}{1 + \beta_1 F + \beta_2 F^2 + \beta_3 F^3 + \beta_4 F^4 + \beta_5 F^5} \quad (10)$$

$$\beta_n = K_{a1}...K_{an}$$

where F represents the concentration of free (unbound) GdL ($Gd(C_{11}\text{-DOTP})^{5-}$). The experimental binding data (up to $\bar{n} = 4$, 42 data points) were fitted to eq 10, and the stoichiometric binding constants K_{a1} to K_{a5} were evaluated (Table 2). The data at $\bar{n} > 4$ were excluded from the fitting as these data points exhibited the highest experimental error and this small number of data points (10) defined four additional binding constants. Including these points and adding additional stoichiometric binding constants (up to K_{a9}) resulted in meaningless parameters with large, indeterminate errors.

Table 2. Association Constants for Binding of Laurate ($C_{11}\text{-}CO_2^-$) versus $Gd(C_{11}\text{-DOTP})^{5-}$ to HSA

binding constant	laurate[a]	$Gd(C_{11}\text{-DOTP})^{5-}$
K_{a1}	$2.40 \times 10^6\ M^{-1}$	$1.27\ (0.30)^b \times 10^5\ M^{-1}$
K_{a2}	$1.10 \times 10^6\ M^{-1}$	$1.94\ (0.89) \times 10^4\ M^{-1}$
K_{a3}	$4.9 \times 10^5\ M^{-1}$	$8.7\ (6.8) \times 10^3\ M^{-1}$
K_{a4}	$2.5 \times 10^5\ M^{-1}$	$2.9\ (3.7) \times 10^3\ M^{-1}$
K_{a5}	$1.9 \times 10^5\ M^{-1}$	$2.7\ (3.1) \times 10^3\ M^{-1}$

[a] Data from Ashbrook, J. D.; Spector, A. A.; Santos, E. C.; Fletcher, J. E. *J. Biol. Chem.* **1975**, *250*, 2333−2338. [b] Values in parentheses represent 1 standard deviation.

Displacement of fluorescent DS from HSA by $Gd(C_{11}\text{-DOTP})^{5-}$ was also studied. DS binds to site II on HSA, the same region of the protein that binds the drugs ibuprofen and diazepam.[28,29] Titration of a DS−HSA solution with $Gd(C_{11}\text{-DOTP})^{5-}$ yielded an inhibition constant, K_i, of 64 μM (Figure 3). As the first two stepwise dissociation constants, determined from the data of Figure 2, were 7.9 and 51 μM ($K_d = 1/K_a$), one interpretation of the fluorescence data is that GdL binds first to a higher affinity site before binding to site II. Displacement of DS then occurs either due to direct competition of $Gd(C_{11}\text{-DOTP})^{5-}$ and DS for site II or possibly by binding of $Gd(C_{11}\text{-DOTP})^{5-}$ to other sites that alters the affinity of HSA for DS at site II.

Water relaxation rate measurements were made at 37 °C on the solutions used in the binding study. Since the free, $[\text{GdL}]_f$, and bound, $[\text{GdL}]_b$, concentrations are directly determined in the ultrafiltration study, it is possible to calculate a mean bound relaxivity, $\bar{r}_{1b}$.

$$\bar{r}_{1b} = \frac{1/T_1^{obs} - 1/T_1^{dia} - [\text{GdL}]_f r_{1f}}{[\text{GdL}]_b} \quad (11)$$

The diamagnetic relaxation rates were measured at each HSA concentration, as these could be HSA dependent. If binding to HSA places $Gd(C_{11}\text{-DOTP})^{5-}$ in the same physicochemical environment (same exposure to water and same rotational correlation times) regardless of the number of $Gd(C_{11}\text{-DOTP})^{5-}$ complexes bound to HSA, then $\bar{r}_{1b}$ should be constant. The mean bound relaxivity is plotted in Figure 4 as a function of unbound

(27) Klotz, I. M. *Ligand Receptor Energetics—A Guide for the Perplexed*; John Wiley & Sons: New York, 1987.
(28) Sudlow, G.; Birkett, D. J.; Wade, D. N. *Mol. Pharmacol.* **1975**, *11*, 824−832.
(29) Sudlow, G.; Birkett, D. J.; Wade, D. N. *Mol. Pharmacol.* **1976**, *12*, 1052−1061.

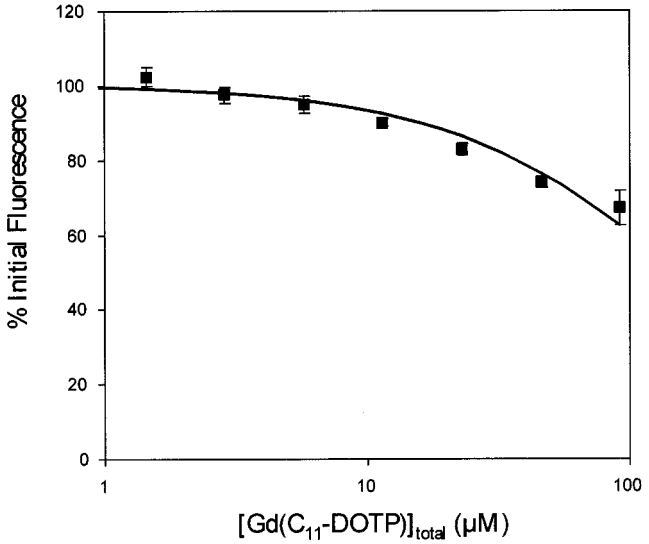

Figure 3. Displacement of binding site II probe DS by $Gd(C_{11}\text{-}DOTP)^{5-}$. Decrease in fluorescence intensity of a 5 μM DS, 5 μM non-defatted HSA solution as a function of $Gd(C_{11}\text{-}DOTP)^{5-}$ added at 37 °C.

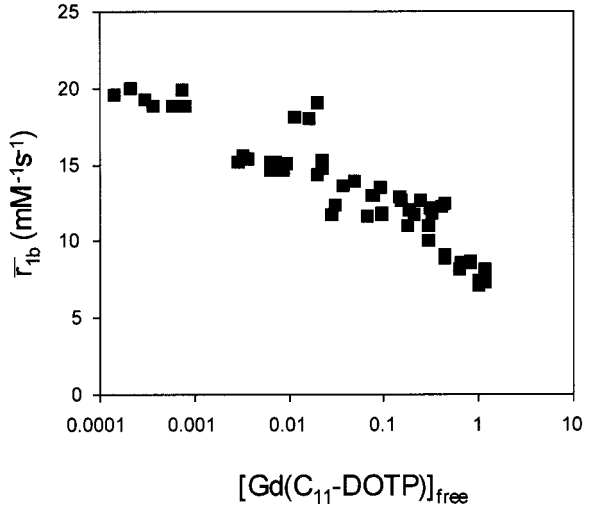

Figure 4. The mean bound relaxivity, $\bar{r}_{1b}$, as a function of unbound $Gd(C_{11}\text{-}DOTP)^{5-}$ determined at 37 °C and 20 MHz. $\bar{r}_{1b}$ is calculated using the binding data from Figure 2 and T_1 values measured on these samples. Note that $\bar{r}_{1b}$ decreases as site occupancy increases.

$[Gd(C_{11}\text{-}DOTP)]^{5-}$. A comparison of Figures 2 and 4 illustrates that the bound relaxivity of $Gd(C_{11}\text{-}DOTP)^{5-}$ depends upon the amount bound to HSA, implying that different binding sites exhibit different relaxivities. This is an insightful result. The PRE method has often been used to determine binding constants of small Gd chelates to albumin.[30−32] One of the normal assumptions made is that there are *n* equivalent binding sites with identical bound relaxivities. The current data show that, at least for $Gd(C_{11}\text{-}DOTP)^{5-}$, there are numerous binding sites and the relaxivity of $Gd(C_{11}\text{-}DOTP)^{5-}$ differs from site to site.

NMRD. In order to ascertain some of the molecular parameters influencing relaxation in the highest affinity site, the relaxivity of $Gd(C_{11}\text{-}DOTP)^{5-}$ was measured as a function of magnetic field under conditions where $Gd(C_{11}\text{-}DOTP)^{5-}$ is predominantly bound to the first site (0.1 mM complex, 4.5% HSA; ~6.7-fold excess protein over complex). The nuclear magnetic relaxation dispersion (NMRD) profile of $Gd(C_{11}\text{-}DOTP)^{5-}$ in the presence (Figures 5 and 6) and absence (Figure S1 of Supporting Information) of 4.5% HSA was recorded at 5, 15, 25, and 35 °C. The relaxivity was determined by subtracting the relaxation rate of the buffer solution (PBS) from the observed relaxation rate (4.5% HSA in PBS) and dividing this difference by the gadolinium concentration. Two things are immediately apparent from the data of Figure 5: the water relaxivity of $Gd(C_{11}\text{-}DOTP)^{5-}$ is greatly enhanced in the presence of HSA (as with BSA, Figure 1), and the relaxivity increases as the temperature decreases. The first result suggests that there is something in addition to diffusion-controlled relaxation that gives the HSA-bound $Gd(C_{11}\text{-}DOTP)^{5-}$ solutions a much higher relaxivity. Relaxation by diffusion is dependent upon the sum of the diffusion coefficients of the water molecule and the paramagnetic molecule.[33] Since water diffuses so much

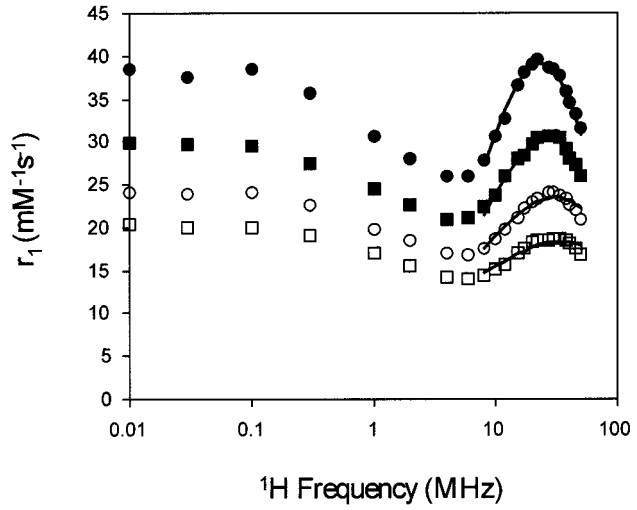

Figure 5. ^1H NMRD of $Gd(C_{11}\text{-}DOTP)^{5-}$ at 5 (●), 15 (■), 25 (○), and 35 (□) °C in the presence of 4.5% non-defatted HSA. The solid lines through the data at high field are the result of the simultaneous fit of all the high-field data to five parameters as outlined in Results.

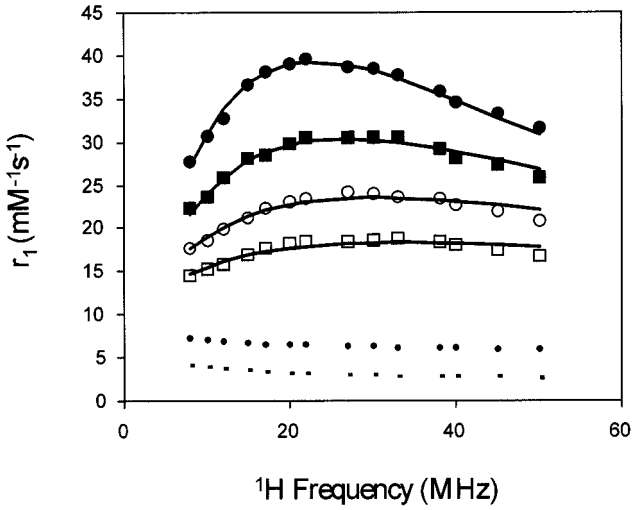

Figure 6. High-field region of NMRD of $Gd(C_{11}\text{-}DOTP)^{5-}$ at 5 (●), 15 (■), 25 (○), and 35 (□) °C in the presence of 4.5% non-defatted HSA. Solid lines represent a fit to the data given by the parameters in Table 3. The dashed lines represent the contributions of translational diffusion to observed relaxivity at 5 (···) and 35 (- - -) °C.

(30) Aime, S.; Botta, M.; Fasano, M.; Crich, S. G.; Terreno, E. *J. Biol. Inorg. Chem.* **1996**, *1*, 312−319.
(31) Muller, R. N.; Radüchel, B.; Laurent, S.; Platzek, J.; Piérart, C.; Mareski, P.; Vander Elst, L. *Eur. J. Inorg. Chem.* **1999**, 1949−1955.
(32) Vander Elst, L.; Maton, F.; Laurent, S.; Seghi, F.; Chapelle, F.; Muller, R. N. *Magn. Reson. Med.* **1997**, *38*, 604−614.
(33) Bertini, I.; Luchinat, C. *Coord. Chem. Rev.* **1996**, *150*, 1−295.

faster than large molecules, the sum of the diffusion coefficients is approximately that of the diffusion coefficient of water. Upon binding to albumin, the diffusion coefficient of the paramagnetic species becomes even smaller relative to that of water. If translational diffusion were the sole determinant of relaxivity, one would not expect it to be dependent upon protein binding. The temperature dependence implies that the observed relaxivity is not limited by the catalytic turnover of water molecules relaxed by the Gd(III) ion. As the solution is cooled, the rate at which relaxed water molecules exchange with unrelaxed water in the bulk solvent slows. At some limiting temperature, this rate of exchange will limit the relaxation enhancement transmitted to the bulk solvent. However, this temperature is not reached in this study.

The parent $LnDOTP^{5-}$ chelates have been widely studied for a number of different lanthanide ions. It is known that $LnDOTP^{5-}$ is quite basic and the predominant species[15] at pH 7.4 is $HLnDOTP^{4-}$. In addition, the thulium complex has been shown to have a high affinity for Ca^{2+}, Mg^{2+}, and Na^{+} and can bind at least three Na^{+} ions[34] with affinities ranging from 10 to 100 M^{-1}. Given that $Gd(C_{11}\text{-DOTP})^{5-}$ lacks an inner-sphere water molecule in water or PBS, it is reasonable to assume that the complex also lacks an inner-sphere water molecule when bound to HSA and that the relaxivity of the HSA-bound species arises from long-lived water molecules in the second sphere or from prototropic exchange between $HGd(C_{11}\text{-DOTP})^{4-}$ (where H represents a proton at an uncoordinated phosphonate oxygen atom) and protons of bulk water solvent. Given this model, NMRD data was treated as follows: first, the observed relaxivity was factored into two components, one for second sphere water protons with residency times (τ_m) longer than the diffusional correlation time (τ_D) and one for relaxation that is defined by translational diffusion, eq 12.

$$r_1 = \frac{q/[H_2O]}{T_{1m} + \tau_m} + C[3j(\omega_I) + 7j(\omega_s)] \tag{12}$$

For second sphere relaxation, it is assumed that there are q water molecules residing at a mean distance, r, from the Gd^{3+} ion, and the relaxation rate of these water molecules is governed by a correlation time, τ_c, eq 13.

$$\frac{1}{T_{1m}} = \frac{2}{15}\left(\frac{\mu_0}{4\pi}\right)^2 \frac{\gamma_H{}^2 g_e{}^2 \mu_B{}^2 S(S+1)}{r_{GdH}{}^6}\left[\frac{3\tau_c}{1+\omega_H{}^2\tau_c{}^2}\right] \tag{13}$$

$$\frac{1}{\tau_c} = \frac{1}{\tau_R} + \frac{1}{\tau_m} + \frac{1}{T_{1e}} \tag{14}$$

Diffusion-controlled relaxation is given by the usual equations (eqs 12, 15−17).

$$C = \left(\frac{32N_A\pi}{405}\right)\left(\frac{\mu_0}{4\pi}\right)^2 \frac{\gamma_I{}^2\gamma_s{}^2\hbar^2 S(S+1)}{aD} \tag{15}$$

$$j(\omega) = \mathrm{Re}\{\{1 + {}^1/_4[i\omega\tau_D + (\tau_D/T_{1e})]^{1/2}\}/\{1 + [i\omega\tau_D + (\tau_D/T_{1e})]^{1/2} + {}^4/_9[i\omega\tau_D + (\tau_D/T_{1e})] + {}^1/_9[i\omega\tau_D + (\tau_D/T_{1e})]^{3/2}\}\} \tag{16}$$

$$\tau_D = a^2/D \tag{17}$$

The diffusional correlation time was fixed to that of water with a distance of closest approach, a, set to 3.8 Å. Both relaxation due to diffusion and relaxation of second sphere water molecules depend on the Gd^{3+} relaxation time, T_{1e}. Equation 18 was used to define the field dependence of T_{1e}.

$$\frac{1}{T_{1e}} = \frac{\Delta^2[4S(S+1)]}{25}\left[\frac{\tau_v}{1+\omega_s{}^2\tau_v{}^2} + \frac{4\tau_v}{1+4\omega_s{}^2\tau_v{}^2}\right] \tag{18}$$

The very low field data points (>4 MHz) were not fitted since gadolinium complexes have a small degree of static zero field splitting. At some point, this zero field splitting energy will become comparable to, and perhaps greater than, the Zeeman energy, and the Solomon−Bloembergen equations will not be valid.[33] By limiting the analysis to the high-field data, the simpler eq 13 is used and there is no dependence on T_{2e} (the component dependent on ω_s has dispersed).

It is assumed that the correlation times τ_R, τ_m, and τ_v have exponential temperature dependencies, eqs 19−21.

$$\tau_R = \tau_R{}^{308}\exp\left[\frac{E_R}{R}\left(\frac{1}{T} - \frac{1}{308.15}\right)\right] \tag{19}$$

$$\frac{1}{\tau_m} = k_{ex} = \frac{k_B T}{h}\exp\left[\frac{\Delta S^{\ddagger}}{R} - \frac{\Delta H^{\ddagger}}{RT}\right] = \frac{T}{\tau_m{}^{310}308.15}\left[\frac{\Delta H^{\ddagger}}{R}\left(\frac{1}{308.15} - \frac{1}{T}\right)\right] \tag{20}$$

$$\tau_v = \tau_v{}^{308}\exp\left[\frac{E_v}{R}\left(\frac{1}{T} - \frac{1}{308.15}\right)\right] \tag{21}$$

It is clear from eqs 12 and 13 that, if $\tau_m \ll T_{1m}$, then q and r are correlated, and only the q/r^6 ratio can be determined. The data for the four temperatures was fitted simultaneously to q/r^6, $\tau_m{}^{308}$, $\Delta H^{\ddagger}$, $\tau_R{}^{308}$, ΔE_R, $\tau_v{}^{308}$, ΔE_v, and Δ^2 using eqs 12−21. The rotational correlation time, τ_R, is long compared to the residency time, τ_m. Since the correlation time, τ_c, depends on the shortest correlation time, τ_R could not be determined accurately. It was also noted that the data fit well without a significant temperature dependence on τ_v, a point noted in other Gd^{3+} NMRD studies.[6] The data (64 points) were then refitted to five parameters: q/r^6, $\tau_m{}^{308}$, $\Delta H^{\ddagger}$, τ_v, and Δ^2, and the results are shown in Table 2. These parameters reproduced the observed relaxivity curves at all four temperatures quite well (Figure 5; an expanded plot of the high-field data and fitted curves is given in Figure 6). The dashed lines in Figures 5 and 6 represent the contribution of translational diffusion to the observed relaxivity at 5 and 35 °C.

While the NMRD of $Gd(C_{11}\text{-DOTP})^{5-}$ bound to HSA is ambiguous with respect to the number of long-lived water molecules (or protons) and their distance of closest approach to the Gd^{3+} ion, it is clear that there is a long correlation time associated with this compound. A residency time of 1 ns at 35 °C accounts for the relatively high relaxivity of an "outer-sphere" compound. By cooling the solution to 5 °C, the residency time increases to 2.6 ns and the relaxivity increases to 40 $mM^{-1}\ s^{-1}$ at 20 MHz. Values of r for various q are also given in Table 3. This result shows how second sphere relaxivity can provide a large boost to observed relaxivity if long-lived water molecules can get close enough to the Gd^{3+} ion, or if the complex can bind several water molecules at once for a lifetime on the order of nanoseconds. There may be long-lived water molecule(s) associated with $Gd(C_{11}\text{-DOTP})^{5-}$ in the absence of HSA. The relaxation data do not allow this distinction. For

(34) Ren, J.; Sherry, A. D. *Inorg. Chim. Acta* **1996**, *246*, 331−341.

Table 3. Parameters Obtained from the Variable-Temperature NMRD Fitting

τ_m^{308} (ns)	1.06 (0.05)[a]	Δ^2 (10^{18} s^{-2})	4.4 (0.1)
$\Delta H^{\ddagger}$ (kJ mol^{-1})	22.3 (0.7)	r (Å), $q = 1$	3.49 (1)
$\Delta S^{\ddagger}$ (J K mol^{-1})	−1 (1)	r (Å), $q = 2$	3.92 (1)
τ_v (ps)	23 (3)	r (Å), $q = 3$	4.19 (1)

[a] Values in parentheses represent 1 standard deviation.

Gd(C_{11}-DOTP)$^{5-}$ in PBS, the rotational correlation time will be on the order of 100−500 ps over this temperature range. If there are water molecule(s) with long residency times (>1 ns), then the correlation time, τ_c, will be determined by rotation, and no insight can be gained into τ_m.

Discussion

Serum albumin binds and transports many exogenous and endogenous ligands, including fatty acids, metal ions, and pharmaceuticals.[35,36] HSA consists of three structurally homologous domains (I, II, and III) that assemble to form a heart-shaped molecule. Each domain is composed of two subdomains (A and B) that possess common structural elements. The hydrophobic pockets or cavities formed by the amino acid residues are responsible for ligand binding,[37] although the number and exact location of the binding sites are still under investigation. It is generally accepted that there are two principal binding areas in subdomains of IIA and IIIA for small heterocyclic or aromatic carboxylic acids and two to three long-chain fatty acid binding sites possibly located in the subdomains of IB, IIIA, and IIIB.[36] Recent X-ray crystal structure of HSA-myristate in the presence of 12-fold excess myristate revealed six fatty acid binding sites located in IA (1), IB (1), IIIA (2), IIIA (1), with the last one belted in the interface of IIA and IIB.[38,39] BSA has structure, amino acid sequence, and binding site locations very similar to those of HSA.[40]

Gd(C_{11}-DOTP)$^{5-}$ shares a common structural feature with fatty acids in having a charged headgroup and an aliphatic side chain. Recently, a derivative of GdDOTA$^-$ having a single dodecyl side chain[41] was shown to form micelles in water above 0.35 mM. The r_1 of the micelles formed by Gd(C_{12}-DOTA)$^-$ was 18 mM^{-1} s^{-1} at 20 MHz and 25 °C.[41] Interestingly, the relaxivity data presented in Figure 1 suggests that Gd(C_{11}-DOTP)$^{5-}$ does not self-associate below 20 mM, likely due to the more highly charged phosphonate headgroup in this molecule. One would anticipate, however, that this complex might bind to multiple fatty acid binding sites on HSA. It has been shown that laurate (equivalent number of saturated carbons) does not saturate HSA even with 9 equiv bound.[42,43] We have shown here that HSA can bind at least five Gd(C_{11}-DOTP)$^{5-}$ complexes, with binding constants ranging from 1.27×10^5 to 2.7×10^3 M^{-1}. In comparison, the six binding constants reported for laurate range from 2.40×10^6 to 6.2×10^4 M^{-1}. Assuming that laurate and Gd(C_{11}-DOTP)$^{5-}$ bind at identical sites, this comparison indicates that the more highly charged chelate headgroup destabilizes binding of the long-chain alkyl group to the fatty acid binding sites on albumin. This likely reflects the greater negative charge that builds on the protein surface as more Gd(C_{11}-DOTP)$^{5-}$ versus laurate is bound. Binding of Gd(C_{11}-DOTP)$^{5-}$ to HSA is however typical of fatty acid type molecules in that several equivalents of fatty acid can be accommodated by the protein.

In another parallel with the fatty acid binding literature, the length of the alkyl chain is critical for albumin binding. The affinity of the octyl analogue, Gd(C_8-DOTP)$^{5-}$, for binding sites on either BSA or HSA is significantly lower than that of Gd(C_{11}-DOTP)$^{5-}$ (Table 1), consistent with the known order of fatty acid binding to albumin, long chain > medium chain > short chain.[35] For both complexes, the affinity for non-defatted HSA was higher than for defatted BSA. The origin of this difference is unclear. The observed relaxivity of Gd(C_8-DOTP)$^{5-}$ was equivalent in the presence of either defatted BSA or non-defatted HSA while the bound relaxivity of Gd(C_{11}-DOTP)$^{5-}$ was higher with defatted BSA than non-defatted HSA. The relaxivity (both observed and calculated bound relaxivity) of Gd(C_{11}-DOTP)$^{5-}$ was higher in the presence of defatted BSA (Table 1). It is known that the conformation of albumin changes dramatically upon fatty acid binding[36] so protein conformation clearly plays a key role in both the affinity and the ability to immobilize a complex to yield a high relaxivity entity. For the two molecules described here, affinity does not correlate with relaxivity. The presence of native fatty acids enables HSA to bind the phosphonate complexes more strongly; however, the relaxivity of the complexes bound to HSA is lower than in the absence of native fatty acids.

As might be expected, HSA has a higher affinity for Gd(C_{11}-DOTP)$^{5-}$ than other low molecular weight, unsubstituted Gd^{3+} chelates. For example, the binding constant for GdDOTP^{5-} with HSA is 3.1×10^3 M^{-1} ($n = 1$)[44] while GdPCTP-[13]$^{3-}$, a triphosphonate complex with a single inner-sphere coordinated water molecule, binds with even lower affinity, 6×10^2 M^{-1} ($n = 1$).[44] Both of these complexes are thought to interact with HSA only through electrostatic interactions with charged groups on the protein surface.[44] Even Gd^{3+} chelates with hydrophobic groups designed to target HSA have more modest binding constants than Gd(C_{11}-DOTP)$^{5-}$. For example, GdDOTA(BOM)$_3^-$ (where BOM = benzyloxymethyl) has a $K_a = 1.7 \times 10^3$ M^{-1} ($n = 2$),[30] GdDTPA(BOM)$_3^-$ has a $K_a = 4 \times 10^4$ M^{-1} (assuming $n = 1$),[45] and MS-325, an agent under commercial development as a blood pool agent, has a $K_{a1} = 1.1 \times 10^4$ M^{-1}.[8]

The relaxivity of Gd(C_{11}-DOTP)$^{5-}$ bound to albumin is remarkably high for a $q = 0$ compound. The relaxivity at 37 °C in HSA is greater than that of a large number of macromolecular $q = 1$ conjugates that have been examined as potential blood pool agents.[45−53] Although the relaxivity at physiological

(35) Peters, T. *All About Albumin: Biochemistry, Genetics and Medical Applications*; Academic Press: San Diego, CA, 1995.
(36) Carter, D. C.; Ho, J. X. *Adv. Protein Chem.* **1994**, *45*, 152−203.
(37) He, X. M.; Carter, D. C. *Nature* **1992**, *358*, 209−215.
(38) Curry, S.; Mandelkow, H.; Brick, P.; Franks, N. *Nat. Struct. Biol.* **1998**, *5*, 827−835.
(39) Curry, S.; Brick, P.; Franks, N. P. *Biochim. Biophys. Acta* **1999**, *1441*, 131−140.
(40) Hamilton, J. A.; Era, S.; Bhamidipati, S. P.; Reed, R. G. *Proc. Natl. Acad. Sci. U.S.A.* **1991**, *88*, 2051−2054.
(41) André, J. P.; Tóth, E.; Fischer, H.; Seelig, A.; Mäcke, H. R.; Merbach, A. E. *Chem. Eur. J.* **1999**, 2977−2983.
(42) Brodersen, R.; Honoré, B.; Pedersen, A. O.; Klotz, I. M. *Trends Pharmacol. Sci.* **1988**, *9*, 252−257.
(43) Pedersen, A. O.; Hust, B.; Andersen, S.; Nielsen, F.; Brodersen, R. *Eur. J. Biochem.* **1986**, *154*, 545−552.
(44) Aime, S.; Botta, M.; Crich, S. G.; Giovenzana, G. B.; Pagliarin, R.; Piccinini, M.; Sisti, M.; Terreno, E. *JBIC, J. Biol. Inorg. Chem.* **1997**, 2, 470−479.
(45) Aime, S.; Chiaussa, M.; Digilio, G.; Gianolio, E.; Terreno, E. *J. Biol. Inorg. Chem.* **1999**, *4*, 766−774.
(46) Bogdanov, A. A.; Weissleder, R.; Frank, H. W.; Bogdanova, A. V.; Nossif, N.; Schaffer, B. K.; Tsai, E.; Papisov, M. I.; Brady, T. J. *Radiology* **1993**, *187*, 701−706.
(47) Bogdanov, A. A. J.; Weissleder, R.; Brady, T. J. *Adv. Drug Delivery Rev.* **1995**, *16*, 335−348.
(48) Desser, T.; Rubin, D.; Muller, H.; Qing, F.; Khodor, S.; Zanazzi; Young, S.; Ladd, D.; Wellons, J.; Kellar, K.; Toner, J.; Snow, R. *J. Magn. Reson. Imaging* **1994**, *4*, 467−472.

temperature is not as high as that of some other albumin-bound blood pool agents (for example, the r_{1b} values of MS-325, $GdDOTA(BOM)_3^-$, and $GdDTPA(BOM)_3^{2-}$ are ~51, ~53, and ~43 mM^{-1} s^{-1}, respectively[7−9,30,45]), it is substantial. The NMRD analysis is consistent with the source of this high relaxivity stemming from water proton(s) with long residency times in the vicinity of the Gd(III) ion. This result may represent a new paradigm in the design of contrast agents for MRI. Lowering the temperature to 5 °C increased r_1 to ~40 mM^{-1} s^{-1}. This suggests that the hydration of $Gd(C_{11}\text{-DOTP})^{5-}$ when bound to albumin is approaching an optimum proton residency time. If this residency time can be lengthened at 37 °C by somehow altering the molecular properties of the complex, then even higher relaxivities would result.

Our binding data also demonstrate that the r_{1b} of $Gd(C_{11}\text{-DOTP})^{5-}$ varies with site occupancy. In the few Gd^{3+} chelates studied that do bind to multiple sites on HSA, a constant r_{1b} is typically assumed when analyzing relaxivity data. The ultrafiltration experiments described here allowed us to directly measure r_{1b} of the bound form of $Gd(C_{11}\text{-DOTP})^{5-}$. These data show quite clearly that either the relaxivity of each site is uniquely different or the relaxivity of one site is altered upon occupancy of subsequent sites. One interpretation of the data shown in Figure 4 ($\bar{r}_{1b}$ decreases with increasing site occupancy) is that less water reaches the second coordination sphere of $Gd(C_{11}\text{-DOTP})^{5-}$ bound at the weaker sites. This is not a physically realistic model, however, because this would imply a stronger interaction between the charged headgroup of $Gd(C_{11}\text{-DOTP})^{5-}$ and the protein surface when it is bound in a weak site versus a stronger binding site. A more reasonable interpretation is that $Gd(C_{11}\text{-DOTP})^{5-}$ is more loosely held in the weaker sites so the correlation time that governs T_{1M} has less contribution from τ_R of the protein.

Acknowledgment. Support for this research was provided in part by grants from the Robert A. Welch Foundation (AT-584), the National Institutes of Health (CA-84697), and the Division of Research Resources, National Institutes of Health (RR-02584). Marga Spiller, New York Medical College, is thanked for recording the NMRD profiles. Dr. Andrew Kolodziej is thanked for the fluorescent probe displacement result.

Supporting Information Available: Figure S1 showing ^1H NMRD curves of $Gd(C_{11}\text{-DOTP})^{5-}$ at 5 (●), 15 (■), 25 (○), and 35 (□) °C in phosphate buffered saline (no albumin present). This material is available free of charge via the Internet at http://pubs.acs.org.

IC0102900

(49) Frank, H.; Weissleder, R.; Bogdanov, A.; Brady, T. *Am. J. Radiol*. **1994**, 1041−1046.
(50) Kellar, K. E.; Henrichs, P. M.; Hollister, R.; Koenig, S. H.; Eck, J.; Wei, D. *Magn. Reson. Med*. **1997**, *38*, 712−716.
(51) Schuhmann-Giampieri, G.; Schmitt-Willich, H.; Frenzel, T.; Press, W. R.; Weinmann, H. *J. Invest. Radiol*. **1991**, *26*, 969−974.
(52) Sieving, P. F.; Watson, A. D.; Rocklage, S. M. *Bioconjugate Chem.* **1990**, *1*, 65−71.
(53) Spanoghe, M.; Lanens, D.; Dommisse, R.; Van der Linden, A.; Alder Weireldt, F. *Magn. Reson. Imaging* **1992**, *10*, 913−917.